

Raman-scattering study of GaP/InP strained-layer superlattices

M. I. Alonso, P. Castrillo, G. Armelles, A. Ruiz, M. Recio, and F. Briones

Centro Nacional de Microelectrónica, Serrano 144, 28006 Madrid, Spain

(Received 17 July 1991; revised manuscript received 31 December 1991)

We discuss the first-order Raman spectra of short-period GaP/InP strained-layer superlattices grown by atomic-layer molecular-beam epitaxy on {001} GaAs substrates. Experimental spectra are successfully explained and compared to the results of simulations consisting of a linear-chain-method calculation combined with the bond-polarizability model.

I. INTRODUCTION

Strained-layer superlattices (SL's) made up of alternate GaP and InP layers constitute a system where the strain is symmetrized when grown on GaAs substrates. While both components present a large lattice mismatch to GaAs (-3.6% GaP, $+3.8\%$ InP) giving rise to large biaxial deformations in the individual layers, the net value of strain in the whole SL is very small, thus favoring their stability.^{1,2} An incentive for studying GaP/InP SL's consists in their potential applications in optoelectronic devices. They are an advantageous alternative to GaInP alloys.^{3,4} Moreover, strain adds a powerful degree of freedom which introduces additional useful features and can be used as a design parameter.⁵

In the present work, we use Raman scattering to investigate the phonon spectra of GaP/InP SL's. The in-plane extensive (compressive) strain present in the GaP (InP) layers shifts the phonon modes to lower (higher) frequencies with respect to their bulk values. These shifts are of the order of 25 cm^{-1} for both materials, thus causing the flatter LO branch of bulk InP to fall within that of GaP. The lattice dynamics of these SL's reflects then mainly the strain present in the layers. We compare our experiments to simulations of the Raman spectra made using the bond-polarizability model^{6,7} with the eigenvectors obtained from a linear-chain calculation.^{6,7}

II. SAMPLE GROWTH AND STRUCTURAL CHARACTERIZATION

Samples have been grown on {001} GaAs substrates by atomic-layer molecular-beam epitaxy (ALMBE).⁸ After a standard cleaning and oxide desorption procedure, a $0.2\text{-}\mu\text{m}$ -thick GaAs buffer layer is grown by conventional molecular-beam epitaxy at a substrate temperature $T_s \sim 580^\circ\text{C}$, in order to improve the starting surface. Substrate temperature is then lowered to the ALMBE growth temperature, closing the As_4 cell for $T_s < 520^\circ\text{C}$. By proceeding in this way, we preserve the substrate from excess arsenic deposition at low temperature, and a clear 2×4 reconstruction is observed in the reflection high-energy electron-diffraction (RHEED) pattern.

The effusion cells we use for group-V elements are specially designed for pulsed operation and ALMBE growth mode.⁹ The background pressure when closed is about

two orders of magnitude lower than the pulse peak or "on" beam equivalent pressure (BEP). This makes it possible to grow compounds containing As and P in the same growth chamber and within the same growth run.

For the growth of GaP/InP SL's, Ga and In fluxes are alternated according to a desired sequence, while phosphorus is supplied in pulses with a repetition cycle determined by the growth rate of each constituent material. The layers measured in this work have been grown at $T_s = 400^\circ\text{C}$ using P_2 pulses of $\text{BEP} \sim 3 \times 10^{-6}$ Torr with a duration of $\tau \sim 0.2r_g$, r_g being the growth rate determined by the flux of the group-III elements.

Growth is monitored by means of the RHEED pattern and reflectance difference spectroscopy (RDS).¹⁰ For the growth of these SL's we have used the cracking section of the phosphorus cell to ensure that the P_2 species is dominant. In previous growth experiments we have seen that, for the mentioned substrate temperature, the incorporation of phosphorus in the InP layers is defective when using P_4 , whereas it is complete when using P_2 as observed by RDS. During growth of the present samples RDS oscillations of constant amplitude were observed indicating¹¹ that their stoichiometry was preserved throughout. The RHEED patterns of the samples remained streaky with clear specular beam, but a dynamic analysis of the in-plane lattice parameter evolution¹² was not possible in this strain-symmetrized system: A lattice relaxation process should take place after growing hundreds of layers and it is difficult to ensure unperturbed RHEED conditions for such a long time.

X-ray diffraction (XRD) was used to assess the structural quality and parameters (period d and strain ϵ) of the SL's. Clear satellite peaks are observed for all the

TABLE I. Characteristics of our $(\text{GaP})_n/(\text{InP})_m$ SL's, grown on {001} GaAs.

Nominal (n, m)	Period (\AA)	ϵ_{GaP} (%)	ϵ_{InP} (%)	SL thickness (nm)
(2,2)	10.6	-3.6	3.7	200
(2,3)	14.1	-3.5	3.6	250
(2,3)	15.3	-3.8	3.6	50
(3,4)	18.7	-4.0	3.4	250
(3,4)	19.1	-3.8	3.6	50

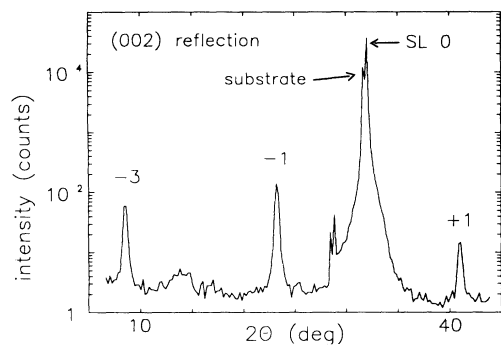


FIG. 1. X-ray spectrum of the $(\text{GaP})_2/(\text{InP})_2$ SL, measured at the (002) reflection.

samples, leading to the periods given in Table I. Figure 1 shows, for example, the rocking curve taken at the (002) reflection of the $(\text{GaP})_2/(\text{InP})_2$ sample. There is an extinction of the satellite -2 because $m = n$, m and n being the number of monolayers of GaP and InP, respectively. The in-plane strain in the individual layers was inferred from measurements by double-crystal XRD of the SLS zeroth-order peak in both the symmetric (004) and asymmetric (511) reflections and the obtained values are quoted in Table I. The mean composition of the samples was checked with microprobe analysis, where it was possible to subtract the contribution of the substrate because there is no As in the SL's. The composition of the layers was found to agree within error with the nominal values.

III. RAMAN MEASUREMENTS

Raman experiments were performed in the back-scattering configuration with incident light polarized parallel to a $\langle 100 \rangle$ axis in the sample. Scattered light was analyzed for polarization, taking spectra polarized both parallel $[z(xx)\bar{z}]$ or perpendicular $[z(xy)\bar{z}]$ to the exciting radiation. The spectra presented in this work were excited by 200 mW of the 514.5-nm line of an argon-ion laser, and the sample was at room temperature. The scattered light was dispersed in a triplemate spectrometer and detected by a charge-coupled device, with a spectral resolution of 4 cm^{-1} and an uncertainty in the frequencies of less than $\pm 1 \text{ cm}^{-1}$.

Figure 2 shows Raman spectra measured in three samples. The spectra of all the studied samples, that are given in Table I, look similar. We could not observe folded acoustic peaks, which may indicate that the photoelastic modulation is small in this highly strained system. We concentrate on the optical region of the spectrum, between 350 and 390 cm^{-1} , where we find the main features of the spectra. The peak observed around 380 cm^{-1} corresponds to the first LO mode confined in the GaP layers. The broader structure centered near 365 cm^{-1} contains one or more modes of different character. We shall return to this assignment in the next section, where a detailed interpretation of the spectra is made with the help of calculations. It must be noticed that these spectra differ from those of unstrained $\text{Ga}_{1-x}\text{In}_x\text{P}$ alloys of cor-

responding compositions,¹³ but they look more similar to those of strained alloys.¹⁴ However, the relative intensities of the peaks observed in the alloy do not change significantly for compositions in the range $x=0.40$ to 0.57 (Ref. 14), while they do in the superlattices, as is observed in Fig. 2. This point will be discussed further in the next section.

We also measured spectra excited with other lines of argon- and krypton-ion lasers covering the visible energy region in order to ensure that the data presented in this work are measured far from any resonances due to electronic transitions. This is important because the relative intensities of both main features in the spectra change with the excitation energy, and then the bond-polarizability model loses its meaning.¹⁵

In the next section we present our modeling of the Raman spectra. We compare the calculations to spectra measured out of resonance, i.e., excited with the laser en-

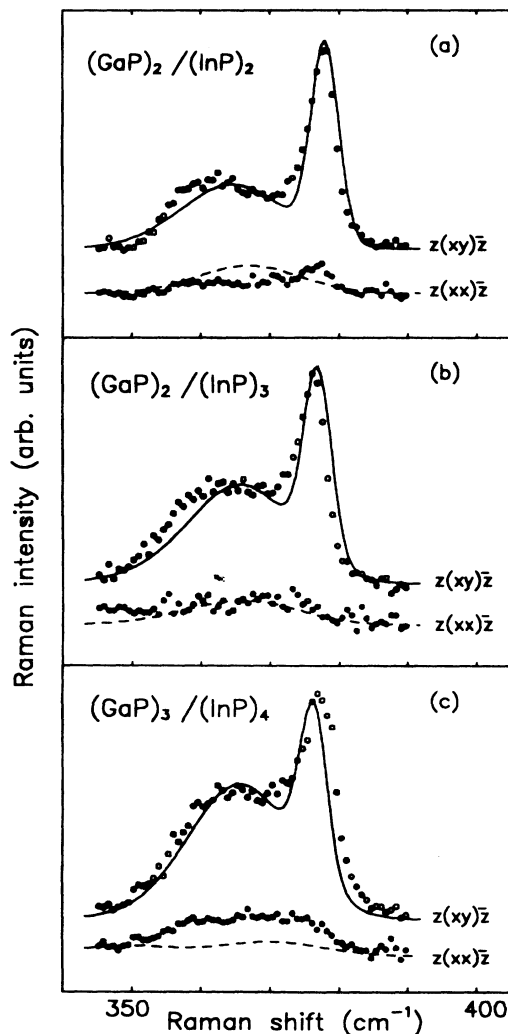


FIG. 2. Raman spectra measured (circles, $\lambda_{\text{exc}} = 514.5 \text{ nm}$) and calculated (lines): (a) $(\text{GaP})_2/(\text{InP})_2$, (b) 50-nm-thick $(\text{GaP})_2/(\text{InP})_3$ SL, and (c) 50-nm-thick $(\text{GaP})_3/(\text{InP})_4$ SL. The origin of differently polarized spectra is shifted for clarity.

ergy farthest from resonant conditions, chosen from our previous measurements to be 514.5 nm (2.41 eV).

IV. MODELING OF THE FIRST-ORDER RAMAN SPECTRA

We calculate the frequencies and eigenvectors of vibrational modes for our SL's using a linear-chain model.^{6,7} By taking only interactions to next-nearest neighbors, the agreement between calculated and experimental values for the dispersion relations of the bulk constituents was rather poor. Hence, as a possible improvement, we have chosen to consider also interactions between second-nearest neighbors. The force constants used in our calculations are $K_{\text{Ga-P}}=102.59$ N/m, $K_{\text{P-P}}=11.15$ N/m, and $K_{\text{Ga-Ga}}=10.34$ N/m for GaP, and $K_{\text{In-P}}=85.52$ N/m, $K_{\text{P-P}}=7.52$ N/m, and $K_{\text{In-In}}=21.55$ N/m for InP. They are fitted to reproduce the experimental^{16,17} LO-phonon frequencies of bulk GaP and InP at the Γ and X points of the Brillouin zone as well as the shape (experimental or result of elaborated calculations)^{16,17} of the optic LO-phonon branch along a $\langle 001 \rangle$ direction.

To transfer this model to the SL structure we introduce the effect of the strain in the force constants of the bulk materials assuming that strain causes the bulk dispersion curves to rigidly shift in the frequency scale. This approximation is reasonable from experimental results; for instance, there is only a small wave-vector dependence in the hydrostatic pressure coefficient of confined LO phonons in GaAs/AlAs superlattices.¹⁸ Also, this approximation was found¹⁹ to be able to account for the phonon frequencies measured²⁰ in GaAs/GaP SL's. A better approach is to consider a scaling law of the force constants, after Cerdeira *et al.*,²¹ as done by Ghanbari *et al.*²² for Si/Ge SL's. The result of this approach is also that strain causes a nearly rigid frequency shift (± 2 cm⁻¹) of the dispersion curves along a $\langle 001 \rangle$ direction.²³

In our calculations we use the known²⁴⁻²⁶ coefficients for the shift of zone-center LO phonons of the bulk constituents to modify the force constants $K_{\text{Ga-P}}$ and $K_{\text{In-P}}$ as

$$K(\epsilon) = K(0)(1 + \sigma\epsilon), \quad (1)$$

where $K(0)$ denotes the force constants for the unstrained case and

$$\sigma = 2 \left[\bar{K}_{12} - \bar{K}_{11} \frac{C_{12}}{C_{11}} \right]. \quad (2)$$

The coefficients \bar{K}_{ij} are defined in Ref. 6 and C_{ij} denote the elastic moduli in standard notation. The values calculated from Eq. (2) are $\sigma_{\text{GaP}}=2.95$ and $\sigma_{\text{InP}}=3.85$. The second-nearest-neighbor force constants are modified in the presence of strain to maintain the shape of the dispersion curve. An average of these constants is taken for interactions across the interfaces.

The optical LO-phonon-dispersion curves along [001] calculated for the strained bulk materials are shown in Fig. 3(a). The value of ϵ used in this case is that given in Table I for the 250-nm-thick (GaP)₂/(InP)₃ SL. The optical dispersion relations along [001] calculated for this sample are displayed in Fig. 3(b). We plot in Fig. 4 the

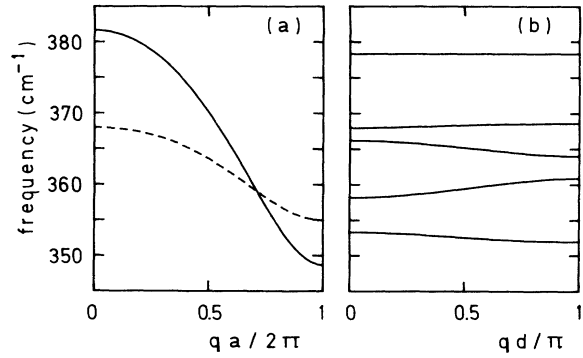


FIG. 3. (a) Optical LO-phonon-dispersion curves along [001] calculated for strained bulk GaP ($\epsilon=-3.5\%$, solid line) and InP ($\epsilon=3.6\%$, dashed line). (b) Optical dispersion relations along [001] calculated for a (GaP)₂/(InP)₃ SL with the same strain values as in (a).

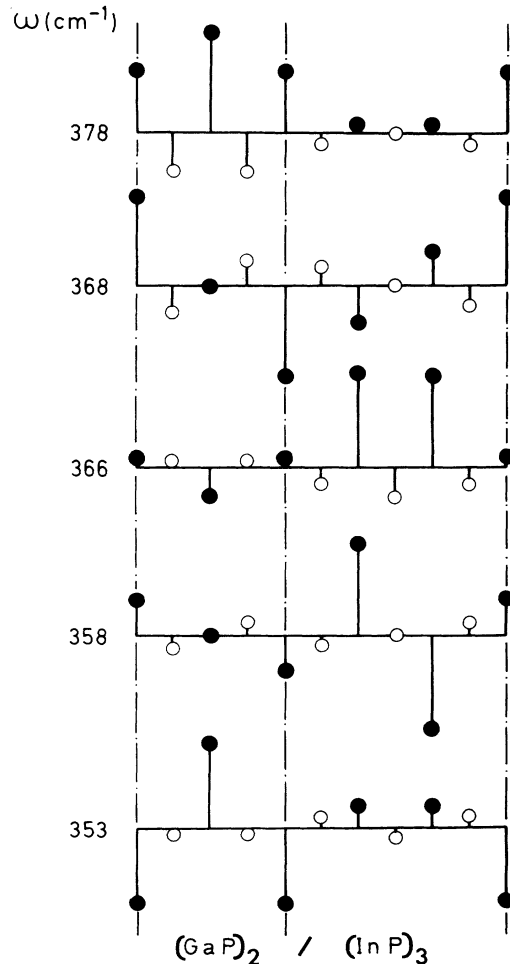


FIG. 4. Atomic displacements for the modes of Fig. 3(b) at $q=0$. Full circles depict P atoms, open circles stay for Ga and In atoms as indicated in the figure.

displacements of the atoms in the unit cell for these modes at $q=0$.

The SL spectrum can be related clearly to the bulk dispersions of the strained bulk constituents. The mode at 378 cm^{-1} is dispersionless, occurring in a frequency range where only vibrational states of bulk GaP are available. The displacement pattern of this mode (see Fig. 4) accordingly shows its amplitude confined in the GaP layers. The dependence of the phonon confinement energy with layer thickness is small for this mode, because the barrier imposed by the vibrational frequencies of InP is low, in a phonon quantum-well picture. Since, in addition, its frequency is very sensitive to the strain present in the GaP layers, it is adequate to use its shift with respect to bulk unstrained GaP to characterize the strain state of the GaP layers, as done in Ref. 3 for $(\text{GaP})_1/(\text{InP})_1$ SL's. The rest of modes have dispersion, and from the displacement patterns plotted in Fig. 4 we see that they have amplitudes in both layers. However, the third displayed mode ($\omega=366\text{ cm}^{-1}$) has its amplitude strongly confined in the InP layers.

Raman intensities in both backscattering configurations are calculated with the bond-polarizability model,^{6,7} using the eigendisplacements resulting from the linear-chain calculation. Each bond is characterized by polarizability parameters α_{xx} and α_{xy} and a factor $\omega^{-1}[1+n(\omega)]$ is taken into account for each frequency.

The spectra calculated for three $(\text{GaP})_n/(\text{InP})_m$ samples with different values of n and m are shown in Fig. 2, together with the experimental data. In order to simulate the measured spectra, the discrete peaks are broadened with a Gaussian line shape having 2-cm^{-1} half-width for the highest-frequency peak and 7.5 cm^{-1} for the other peaks. We choose these values because they yield a good agreement between calculated and measured spectra for all samples. The fact that these widths are different can be a signature of interface roughness, especially because the layers are extremely thin. Interface roughness relaxes the \mathbf{k} -conservation rule and Raman scattering from phonons throughout the SL Brillouin zone is expected. Then, a dispersionless mode will still remain a well-defined peak, while the width of a dispersive mode will be

larger.

Bond polarizabilities have been taken to be equal for both configurations ($\alpha_{xx}=\alpha_{xy}=\alpha$) but a factor of 2.4 larger in InP than in GaP bonds ($\alpha_{\text{InP}}=2.4\alpha_{\text{GaP}}$). This choice gives a remarkably good agreement between measured and calculated $z(xy)\bar{z}$ spectra for all our samples, and it compares well to other cases, as, for example, in GaAs/AlAs superlattices, where $\alpha_{\text{GaAs}}\approx 3\alpha_{\text{AlAs}}$.⁷ The polarizability of the bonds increases also in the sequence of diamond-type crystals C, Si, and Ge.²⁷ Barker, Merz, and Gossard⁷ could find different values for α_{xx} and α_{xy} of GaAs and AlAs bonds. From our experimental data a fit of α_{xx} would be meaningless, the observed $z(xx)\bar{z}$ scattering component out of resonance being very weak (see Fig. 2). It is noticeable that the measured intensities of the peaks in $z(xy)\bar{z}$ configuration are well reproduced by the calculated eigenvectors. The intensities have no direct relation with the mean composition of the samples compared to $\text{Ga}_{1-x}\text{In}_x\text{P}$, being $x=0.50$ ($n=m=2$), $x=0.57$ ($n=3, m=4$), and $x=0.60$ ($n=2, m=3$).

V. CONCLUSIONS

We have investigated the phonon spectra of $(\text{GaP})_n/(\text{InP})_m$ SL's grown on $\{001\}$ GaAs by using Raman spectroscopy. The observed first-order Raman spectra have been successfully explained on the basis of a linear-chain method calculation of the phonon frequencies and their associated eigendisplacements. These have been used to model the Raman intensities by assigning a polarizability to InP bonds 2.4 times larger than that of GaP bonds. The calculated eigenvectors show that the two main features observed in the spectra are due to phonon modes confined in the two types of layers.

ACKNOWLEDGMENTS

We thank A. Mazuelas for providing some double-crystal XRD data and V. Velasco for useful discussions on the phonon calculations.

¹S. M. Bedair, *Cryst. Prop. Prep.* **21**, 119 (1989).

²E. Kasper, H.-J. Herzog, H. Daembkes, and G. Abstreiter, in *Layered Structures and Epitaxy*, edited by J. M. Gibson, G. C. Osbourn, and R. M. Tromp, MRS Symposia Proceedings No. 56 (Materials Research Society, Pittsburgh, 1986), p. 347.

³R. M. Abdelouhab, R. Braunstein, M. A. Rao, and H. Kroemer, *Phys. Rev. B* **39**, 5857 (1989).

⁴B. T. McDermott, K. G. Reid, N. A. El-Mastry, S. M. Bedair, W. M. Duncan, X. Yin, and F. H. Pollak, *Appl. Phys. Lett.* **56**, 1172 (1990).

⁵M. Recio, A. Ruiz, J. Meléndez, J. M. Rodríguez, G. Armelles, M. L. Dotor, and F. Briones, in *Physical Concepts of Materials for Novel Optoelectronic Device Applications I*, edited by M. Razegui (Society of Photo-Optical Instrumentation Engineers, Bellingham, 1991), Vol. 1361, p. 469.

⁶For a review on the subject of Raman spectroscopy of vibra-

tions in superlattices, see B. Jusserand and M. Cardona, in *Light Scattering in Solids V*, edited by M. Cardona and G. Güntherodt (Springer-Verlag, Berlin, 1989), p. 49.

⁷A. S. Barker, Jr., J. L. Merz, and A. C. Gossard, *Phys. Rev. B* **17**, 3181 (1978).

⁸F. Briones, L. González, and A. Ruiz, *Appl. Phys. A* **49**, 729 (1989).

⁹A. Ruiz, F. Briones, G. Armelles, and M. Recio, in *5th European Workshop on Molecular Beam Epitaxy*, edited by G. Weimann, I. Eisele, and H. Schlötterer (Grainau, Germany, 1989).

¹⁰D. E. Aspnes, J. P. Harbison, A. A. Studna, and L. T. Florez, *Appl. Phys. Lett.* **52**, 957 (1988).

¹¹F. Briones and Y. Horikoshi, *Jpn. J. Appl. Phys.* **29**, 1014 (1990).

¹²A. Ruiz, L. González, A. Mazuelas, and F. Briones, *Appl.*

- Phys. A **49**, 543 (1989).
- ¹³E. Bedel, R. Carles, G. Landa, and J. B. Renucci, *Rev. Phys. Appl.* **19**, 17 (1984).
- ¹⁴R. M. Abdelouhab, R. Braunstein, K. Bärner, M. A. Rao, and H. Kroemer, *J. Appl. Phys.* **66**, 787 (1989), and references therein.
- ¹⁵M. Cardona, in *Light Scattering in Solids II*, edited by M. Cardona and G. Güntherodt (Springer-Verlag, Heidelberg, 1982), p. 40.
- ¹⁶L. L. Yarnell, J. L. Warren, R. G. Wenzel, and P. J. Dean, *Neutron Inelastic Scattering* (IAEA, Vienna, 1968), Vol. 1, p. 301.
- ¹⁷P. H. Borchers, G. F. Alfrey, D. H. Saunderson, and A. D. B. Woods, *J. Phys. C* **8**, 2022 (1975); P. H. Borchers, K. Kunc, G. F. Alfrey, and R. L. Hall, *ibid.* **12**, 4699 (1979).
- ¹⁸P. Seguy, J. C. Maan, A. Fasolino, G. Martinez, and K. Ploog, in *Proceedings of the 19th International Conference on the Physics of Semiconductors*, edited by W. Zawadzki (Institute of Physics, Polish Academy of Sciences, Warsaw, 1988), Vol. I, p. 803.
- ¹⁹K. W. Kim, M. A. Strocio, and J. C. Hall, *J. Appl. Phys.* **67**, 6179 (1990).
- ²⁰G. Armelles, M. Recio, A. Ruiz, and F. Briones, *Solid State Commun.* **71**, 431 (1989).
- ²¹F. Cerdeira, F. J. Buchenauer, F. H. Pollak, and M. Cardona, *Phys. Rev. B* **5**, 580 (1972).
- ²²R. A. Ghanbari, J. D. White, G. Fasol, C. J. Gibbings, and C. G. Tuppen, *Phys. Rev. B* **42**, 7033 (1990).
- ²³V. R. Velasco (private communication).
- ²⁴I. Balslev, *Phys. Status Solidi B* **61**, 207 (1974).
- ²⁵E. Anastassakis, Y. S. Raptis, M. Hünnermann, W. Richter, and M. Cardona, *Phys. Rev. B* **38**, 7702 (1988).
- ²⁶B. A. Weinstein and R. Zallen, in *Light Scattering in Solids IV*, edited by M. Cardona and G. Güntherodt (Springer, Heidelberg, 1984), p. 463.
- ²⁷S. Go, H. Bilz, and M. Cardona, *Phys. Rev. Lett.* **34**, 580 (1975).